Proc. 2nd U.S.-Japan Workshop on Soil-Structure Interaction, March 6-8, 2001, Tsukuba City, Japan.

FLEXIBLE VERSUS RIGID FOUNDATION MODELS OF SOIL-STRUCTURE INTERACTION: INCIDENT SH-WAVES

Maria I. Todorovska[1], Abdul Hayir[2] and Mihailo D. Trifunac[3]

Keywords: soil-structure interaction; wave passage effects; differential motion; dynamic interaction; flexible imbedded foundation.

ABSTRACT

A common assumption in modeling soil-structure interaction is that the foundation is rigid. This reduces the complexity of the problem (i.e. the number of additional degrees of freedom for accounting for the interaction), and makes it possible to present general results that can be used for different structures (the substructure approach for linear models). In reality, building foundations are flexible. This paper presents an analysis of the consequences of this assumption, using a simple structural model: an elastic circular wedge supported by a flexible circular foundation embedded into a half-space and excited by incident pane SH-waves. The problem is solved by expansion of the motion in all three media (wedge, foundation and half-space) in cylindrical wave functions (Fourier-Bessel series). The structural model is simple, but accounts for both differential motions of the base and for the effects of soil-structure interaction. Usually, structural models in earthquake engineering consider either differential ground motion, but ignore soil-structure interaction, or consider soil-structure interaction, but for a rigid foundation, thus ignoring differential ground motion. This study attempts to find how stiff the foundation should be relative to the soil so that the rigid foundation assumption in soil-structure interaction models is valid. The shortest wavelength of the incident waves considered in this study is one equal to the width of the base of the wedge. It is concluded that, for this model, a foundation with same mass density as the soil but 50 times larger shear modulus behaves as "rigid". For ratio of shear moduli less than 16, the rigid foundation assumption is not valid. Considering differential motions is important because of additional stresses in structures that are not predicted by fixed-base and rigid foundation models.

1. INTRODUCTION

For structures on multiple supports or on extended flexible foundations, it is important to consider the effects of differential ground motion because of excitation of anti-symmetric modes of vibration and additional stresses (to those predicted by synchronous motion) in the structure due to non-classical "modes" of vibration and quazi-static deformations which are the largest near the base (Todorovska and Lee, 1989; Todorovska and Trifunac, 1989; 1990a,b; Trifunac and Todorovska, 1997). Another consequence of the finite flexibility of the soil is the soil-structure interaction, which refers to modification of the ground motion due to scattering of the incident waves from the foundation and radiation of energy from the structure into the soil. Due to increased complexity of the problem, models usually consider either one of these two effects and ignore the other effect. Studies that include both are rare. For example, Iguchi and Luco (1982) and Liou and Huang (1994) present impedance functions for a flexible circular disk

[1] Research Associate Professor, University of Southern California, Civil Engineering Department, Los Angeles, CA 90089-2531.
[2] Technical University of Istanbul, Civil Engineering Department, Maslak, 80626, Istanbul, Turkey, and Visiting Scholar, University of Southern California, Civil Engineering Department, Los Angeles, CA 90089-2531.
[3] Professor, University of Southern California, Civil Engineering Department, Los Angeles, CA 90089-2531.

foundation with a rigid core (where the forces from the structure are applied) and for in-plane incident waves. They conclude that a consequence of the rigid-foundation assumption is that the radiation damping is exaggerated, in particular for shorter wavelengths of the incident waves.

This paper summarizes the results of Hayir et al. (2001) and Todorovska et al. (2001), who considered a simple structure - a wedge, supported respectively by a half-space but with a flexible interface between the structure and the half-space, or by a flexible foundation embedded into a half-space and excited by plane SH-waves. All the contact surfaces and media are flexible and transmit waves from one medium to the other. This paper attempts to find how stiff a foundation should be relative to the soil for the rigid foundation assumption in similar soil-structure interaction models to be valid.

2. MODEL

The two-dimensional (2D) model consists of a circular wedge, supported by a flexible circular foundation embedded in a half-space. Perfect bond is assumed at the contact surfaces. All the three media are linear, elastic, homogeneous and isotropic, with shear wave velocities and shear moduli β_D, μ_D, β_F, μ_F, β_s and μ_s. Figure 1 shows a vertical cross-section of the model. The wedge has center of curvature at point O_1, radius b_D and angle $2\theta_0$. The boundary between the foundation and the half-space has center of curvature also at O_1, and radius b_F. The model is symmetric about the vertical line through points O and O_1, which are the origins of the two Cartesian coordinate systems, x-y-z and x_1-y_1-z_1, used to describe the motion of the system. Axes y and y_1 project into points on the plane shown in Figure 1 and point towards the reader. Associated to these two Cartesian coordinate systems are cylindrical coordinate systems R-θ-y and R_1-θ_1-y_1 as shown in Figure 1. The distance between the origins of these two coordinate systems is $d = b\cos\theta_0$. The

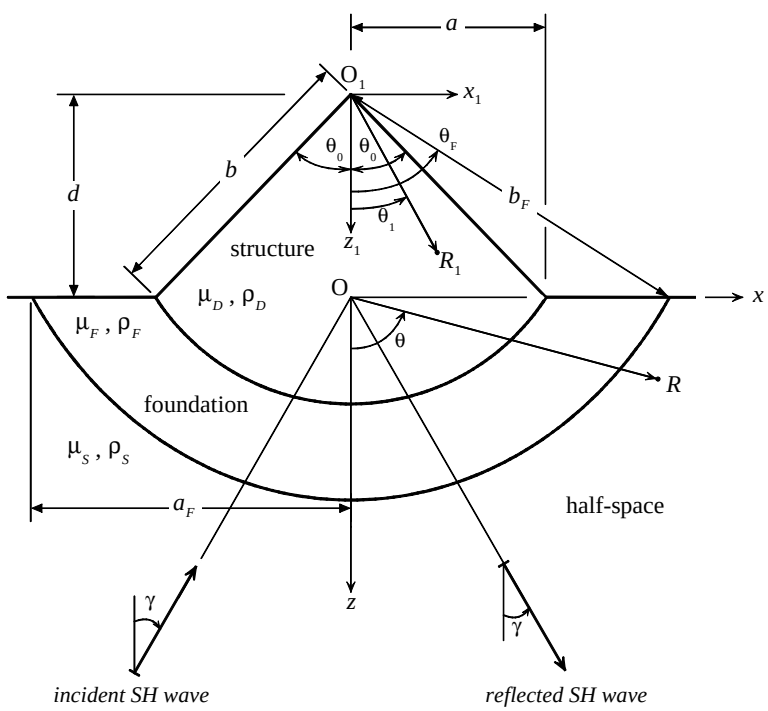

Figure 1 The model.

half-width of the base of the dike is $a = b\sin\theta_0$, and of the foundation is $a_F = b_F \sin\theta_F$, where $\theta_F = \cos^{-1}\dfrac{b\cos\theta_0}{b_F}$. We will use a as characteristic length of the model. The excitation is a plane SH-wave with frequency ω, angle of incidence γ, amplitude u_0, and displacement in the y–direction

$$U^{(i)} = u_0 \exp\left[k_s\left(x\sin\gamma - z\cos\gamma\right) - i\,\omega\, t\right] \tag{1}$$

where t is time and $k_s = \omega/\beta_s$ is the wave number of shear waves in the half-space.

2.1 Equation of Motion and Boundary and Continuity Conditions

The wedge (dike, structure), foundation and half-space will respond by anti-plane motions, $U^{(D)}$, $U^{(F)}$, and $U^{(s)}$, such that they all satisfy the wave equation

$$\frac{\partial^2 U}{\partial x^2} + \frac{\partial^2 U}{\partial z^2} = \frac{1}{\beta^2}\frac{\partial^2 U}{\partial t^2} \tag{2}$$

subject to the following zero-stress boundary conditions

$$\sigma_{\theta y}^{(s)} = 0 \quad \text{at} \quad R > a_F \text{ and } \theta = \pm\frac{\pi}{2} \tag{3}$$

$$\sigma_{\theta y}^{(F)} = 0 \quad \text{at} \quad a < R < a_F \text{ and } \theta = \pm\frac{\pi}{2} \tag{4}$$

$$\sigma_{\theta_1 y}^{(D)} = 0 \quad \text{at} \quad R_1 < b \text{ and } \theta_1 = \pm\theta_0 \tag{5}$$

where

$$\sigma_{\theta y} = \frac{\mu}{R}\frac{\partial U}{\partial \theta} \tag{6}$$

Displacements $U^{(D)}, U^{(F)}$ and $U^{(s)}$ also have to satisfy the continuity of stresses and displacements conditions at the contact surface

$$U^{(D)} = U^{(F)} \quad \text{at } R_1 = b \text{ and } -\theta_0 \le \theta_1 \le \theta_0 \tag{7}$$

$$\sigma_{R_1 y}^{(D)} = \sigma_{R_1 y}^{(F)} \quad \text{at } R_1 = b \text{ and } -\theta_0 \le \theta_1 \le \theta_0 \tag{8}$$

$$U^{(F)} = U^{(s)} \quad \text{at } R_1 = b_F \text{ and } -\theta_F \le \theta_1 \le \theta_F \tag{9}$$

$$\sigma_{R_1 y}^{(F)} = \sigma_{R_1 y}^{(s)} \quad \text{at } R_1 = b_F \text{ and } -\theta_F \le \theta_1 \le \theta_F \tag{10}$$

where

$$\sigma_{R_1 y} = \mu\frac{\partial U}{\partial R_1} \tag{11}$$

2.2 Representation of the Motion in the Half-Space and in the Structure

The motion in the half-space can be represented as a sum of the free-field motion, $U^{(ff)}$, and perturbation, $U^{(R)}$, due to waves scattered from the wedge

$$U^{(s)} = U^{(ff)} + U^{(R)} \tag{12}$$

The free-field motion is the sum of the incident wave, $U^{(i)}$, and the wave $U^{(r)}$ reflected from the half-space surface, if the structure were not there

$$U^{(ff)} = U^{(i)} + U^{(r)} \tag{13}$$

The reflected wave is

$$U^{(r)} = u_0 \exp\left[k_s\left(x\sin\gamma + z\cos\gamma\right) - i\omega t\right]. \tag{14}$$

The free-field motion $U^{(ff)}$ satisfies the zero-stress condition (3). Then, the scattered field must also satisfy the zero-stress condition (3) as well as the wave equation (2), and it should be an outgoing wave. Such motion can be represented by the following Fourier-Bessel series [Trifunac, 1971]

$$U^{(R)}(R,\theta) = u_0 \sum_{n=0}^{\infty}\left[A_n^R H_{2n}^{(1)}(k_s R)\cos 2n\theta + B_n^R H_{2n+1}^{(1)}(k_s R)\sin(2n+1)\theta\right]\exp(-i\omega t) \tag{15}$$

where A_n^R and B_n^R are unknown coefficients and $H_n^{(1)}(.)$ is the Hankel function of the first kind and order *n*. The displacement of the foundation can be represented as

$$\begin{aligned} U^{(F)} = \sum_{n=0}^{\infty}\Big[& A_n^F H_{2n}^{(1)}(k_F R)\cos(2n\theta) + B_n^F H_{2n+1}^{(1)}(k_F R)\sin(2n+1)\theta \\ & + C_n^F H_{2n}^{(2)}(k_F R)\cos(2n\theta) + D_n^F H_{2n+1}^{(2)}(k_F R)\sin(2n+1)\theta \Big]\exp(-i\omega t) \end{aligned} \tag{16}$$

where A_n^F, B_n^F, C_n^F and D_n^R are unknown coefficients and $H_n^{(2)}(.)$ is the Hankel function of the second kind and order *n*. The representation of displacement in the structure that satisfies automatically the zero–stress condition (4) is

$$U^{(D)}(R_1,\theta_1) = u_0 \sum_{n=0}^{\infty}\left\{A_n^D J_{2n}(k_b R_1)\cos\left[2n\frac{\pi}{2\theta_0}\theta_1\right] + B_n^D J_{2n+1}(k_b R_1)\sin\left[(2n+1)\frac{\pi}{2\theta_0}\theta_1\right]\right\}\exp(-i\omega t) \tag{17}$$

where A_n^D and B_n^D are unknown coefficients.

2.3 Solution

The representations of the motions in the structure and in the half-space, i.e. $U^{(ff)}$, $U^{(R)}$ and $U^{(D)}$, are such that the zero-stress conditions on the outer boundaries are automatically satisfied. The unknown coefficients are then determined from the continuity of displacements and stresses conditions (7) through (11). Matching these continuity conditions requires same representation for $U^{(ff)}$, $U^{(R)}$, $U^{(F)}$ and $U^{(D)}$. Such a representation is expansion in Fourier-Bessel series of R_1 and θ_1 with period 2π. We follow the procedure we used in our previous paper on response of a dike to SH-waves where the dike is in direct contact with the half-space (Hayir et al., 2001). To avoid repetition, in the following, we present only the

representations of motion, and expressions that are new or that differ from our earlier paper. The expansions of $U^{(i)}$ and $U^{(r)}$ are

$$U^{(i)} = u_0 \exp(i\, k_s\, d \cos\gamma) \sum_{m=0}^{\infty} \varepsilon_m\, (-i)^m J_m(k_s R_1) \cos m(\theta_1 + \gamma) \exp(-i\,\omega\, t) \tag{18}$$

$$U^{(r)} = u_0 \exp(-i\, k_s\, d \cos\gamma) \sum_{m=0}^{\infty} \varepsilon_m\, (i)^m J_m(k_s R_1) \cos m(\theta_1 - \gamma) \exp(-i\,\omega\, t) \tag{19}$$

where

$$\varepsilon_m = \begin{cases} 1, & m = 0 \\ 2 & m > 0 \end{cases} \tag{20}$$

The representation of transformed $U^{(R)}$ is

$$U^{(R)}(R_1, \theta_1) = u_0 \sum_{m=0}^{\infty} \sum_{n=0}^{\infty} H_m^{(1)}(k_s\, R_1) \left[A_n^R P_{m,n}(k_s d) \cos m\theta_1 + B_n^R Q_{m,n}(k_s d) \sin m\theta_1 \right] \exp(-i\omega t) \tag{21}$$

and of $U^{(F)}$ is

$$\begin{aligned} U^{(F)} = \sum_{m=0}^{\infty} \sum_{n=0}^{\infty} \Big\{ & H_m^{(1)}(k_F\, R_1) \left[A_n^F\, P_{m,n}\,(k_F d) \cos m\theta_1 + B_n^F\, Q_{m,n}\,(k_F d) \sin m\theta_1 \right] \\ & + H_m^{(2)}(k_F\, R_1) \left[C_n^F\, P_{m,n}\,(k_F d) \cos m\theta_1 + D_n^F\, Q_{m,n}\,(k_F d) \sin m\theta_1 \right] \Big\} \exp(-i\,\omega\, t) \end{aligned} \tag{22}$$

where $P_{m,n}\,(s)$ and $Q_{m,n}\,(s)$ are

$$\begin{aligned} P_{m,n}(s) &= \frac{\varepsilon_m}{2} \left[J_{m+2n}(s) + (-1)^{2n}\, J_{m-2n}(s) \right] \\ Q_{m,n}(s) &= \frac{\varepsilon_m}{2} \left[J_{m+2n+1}(s) - (-1)^{2n+1}\, J_{m-2n+1}(s) \right] \end{aligned} \tag{23}$$

The expression for $U^{(D)}$ is transformed by expanding $\cos\left[2n \frac{\pi}{2\theta_0} \theta_1 \right]$ and $\sin\left[(2n+1) \frac{\pi}{2\theta_0} \theta_1 \right]$ in eqn (13) in Fourier series of period 2π. This leads to

$$U^{(D)}(R_1, \theta_1) = u_0 \sum_{m=0}^{\infty} \sum_{n=0}^{\infty} \left[A_n^D\, J_{2n}(k_b R_1) M_{m,n} \cos m\theta_1 + B_n^D\, J_{2n+1}(k_b\, R_1) N_{m,n} \sin m\theta_1 \right] \exp(-i\omega t) \tag{24}$$

where

$$M_{m,n} = \frac{1}{\pi} \int_{-\pi}^{\pi} \cos\left[2n \frac{\pi}{2\theta_0} \theta_1 \right] \cos m\theta_1\, d\theta_1 \tag{25a}$$

$$N_{m,n} = \frac{1}{\pi}\int_{-\pi}^{\pi} \sin\left[(2n+1)\frac{\pi}{2\theta_0}\theta_1\right]\sin m\theta_1 \, d\theta_1 \tag{25b}$$

The above Fourier expansion assumes extension of $U^{(D)}$ beyond the domain of the structure, i.e. on $[-\pi,\pi]$, to minimize the Gibb's effects at $\theta_1 = \pm\theta_0$. After evaluation of the integrals

$$M_{m,n} = \begin{cases} 1, & n = m = 0 \\ 1+\sin\left[4n\pi\dfrac{\pi}{2\theta_0}\right]\Big/\left[4n\pi\dfrac{\pi}{2\theta_0}\right], & m = 2n\dfrac{\pi}{2\theta_0} \\ (-1)^m \sin\left[2n\pi\dfrac{\pi}{2\theta_0}\right]\Big/\left[-\dfrac{m^2\pi}{4n}\left(\dfrac{\pi}{2\theta_0}\right)^{-1} + n\pi\dfrac{\pi}{2\theta_0}\right], & m \neq 2n\dfrac{\pi}{2\theta_0} \end{cases} \tag{26a}$$

$$N_{m,n} = \begin{cases} 0, & n = m = 0 \\ 1-\sin\left[2(2n+1)\pi\dfrac{\pi}{2\theta_0}\right]\Big/\left[2(2n+1)\pi\dfrac{\pi}{2\theta_0}\right], & m = (2n+1)\dfrac{\pi}{2\theta_0} \\ (-1)^m \sin\left[(2n+1)\pi\dfrac{\pi}{2\theta_0}\right]\Big/\left[-\dfrac{m\pi}{2} + \dfrac{(2n+1)^2\pi}{2m}\dfrac{\pi}{2\theta_0}\right], & m \neq (2n+1)\dfrac{\pi}{2\theta_0} \end{cases} \tag{26b}$$

The stresses are

$$\begin{aligned} \sigma_{rz}^{(s)}(R_1,\theta_1) = \frac{\sigma_0}{k_F R_1}\frac{\mu_s}{\mu_F}\sum_{m=0}^{\infty}\sum_{n=0}^{\infty} & A_n^R\, T_m(3, k_s R_1) P_{m,2n}(k_s d)\cos m\theta_1 \\ & + B_n^R T_m(3, k_s R_1) Q_{m,2n+1}(k_s d)\sin m\theta_1 \\ & + T_m(1, k_s R_1)\varepsilon_m (-i)^m \exp(ik_s d\cos\gamma)\cos m(\theta_1+\gamma) \\ & + T_m(1, k_s R_1)\varepsilon_m (i)^m \exp(-ik_s d\cos\gamma)\cos m(\theta_1-\gamma) \end{aligned} \tag{27}$$

$$\begin{aligned} \sigma_{rz}^{(F)}(R_1,\theta_1) = \frac{\sigma_0}{k_F R_1}\sum_{m=0}^{\infty}\sum_{n=0}^{\infty} & A_n^F\, T_{2n}(3, k_D R_1) M_{m,n}\cos m\theta_1 \\ & + B_n^F\, T_{2n+1}(3, k_D R_1) N_{m,n}\sin m\theta_1 \\ & + C_n^F\, T_{2n}(4, k_D R_1) M_{m,n}\cos m\theta_1 \\ & + D_n^F\, T_{2n+1}(4, k_D R_1) N_{m,n}\sin m\theta_1 \end{aligned} \tag{28}$$

$$\sigma_{rz}^{(D)}(R_1,\theta_1) = \frac{\sigma_0}{k_D R_1}\frac{\mu_D}{\mu_F}\sum_{m=0}^{\infty}\sum_{n=0}^{\infty} A_n^D\, T_{2n}(1, k_D R_1) M_{m,n}\cos m\theta_1 + B_n^D\, T_{2n+1}(1, k_D R_1) N_{m,n}\sin m\theta_1 \tag{29}$$

where

$$T_m(j,s) = m\,\Psi_m(s) - s\,\Psi_{m+1}(s), \qquad \Psi_m(s) = \begin{cases} J_m(s), & j=1 \\ Y_m(s), & j=2 \\ H_m^{(1)}(s), & j=3 \\ H_m^{(2)}(s), & j=4 \end{cases} \tag{30}$$

and the normalization stress is

$$\sigma_0 = \mu_F\, k_F u_0 \tag{31}$$

The continuity conditions imply the following system of equations to be solved for the unknown coefficients of expansion of the motion in the half-space, foundation and the wedge,

$$\begin{bmatrix} \cdot & \vdots & \cdot \\ \cdots & \left[W_{m,n}^{sym}\right]_{4\times4} & \cdots \\ \cdot & \vdots & \cdot \end{bmatrix}_{m\times n} \begin{Bmatrix} \vdots \\ \begin{Bmatrix} A_n^R \\ A_n^D \\ A_n^F \\ C_n^F \end{Bmatrix}_{4\times1} \\ \vdots \end{Bmatrix}_{n\times1} = \begin{Bmatrix} \vdots \\ \left\{V_m^{sym}\right\}_{4\times1} \\ \vdots \end{Bmatrix}_{n\times1} \tag{32}$$

where

$$\left[W_{m,n}^{sym}\right]_{4\times4} =$$

$$\begin{bmatrix} 0 & J_{2n}(k_D b) M_{m,n} & -H_m^{(1)}(k_F b) P_{m,n}(k_F d) & -H_m^{(2)}(k_F b) P_{m,n}(k_F d) \\ 0 & T_{2n}(1, k_D b) M_{m,n} & -\dfrac{\mu_f}{\mu_D} T_m(3, k_F b) P_{m,n}(k_F d) & -\dfrac{\mu_f}{\mu_D} T_m(4, k_F b) P_{m,n}(k_F d) \\ -H_m^{(1)}(k_s b_F) P_{m,n}(k_s d) & 0 & H_m^{(1)}(k_F b_F) P_{m,n}(k_F d) & H_m^{(2)}(k_F b_F) P_{m,n}(k_F d) \\ -T_m(3, k_s b_F) P_{m,n}(k_s d) & 0 & \dfrac{\mu_f}{\mu_s} T_m(3, k_F b_F) P_{m,n}(k_F d) & \dfrac{\mu_f}{\mu_s} T_m(3, k_F b_F) P_{m,n}(k_F d) \end{bmatrix}_{4\times4} \tag{33}$$

$$\left\{V_m^{sym}\right\}_{2\times1} = \begin{Bmatrix} 0 \\ 0 \\ \varepsilon_m J_m(k_s b_F) \cos m\gamma \left[(-i)^m \exp(i k_s d \cos\gamma) + i^m \exp(-i k_s d \cos\gamma)\right] \\ \varepsilon_m T_m(1, k_s b_F) \cos m\gamma \left[(-i)^m \exp(i k_s d \cos\gamma) + i^m e^{-i k_s d \cos\gamma} \exp(-i k_s d \cos\gamma)\right] \end{Bmatrix} \tag{34}$$

and

$$\begin{bmatrix} \cdot & \vdots & \cdot \\ \cdots & \left[W_{m,n}^{asym}\right]_{4\times4} & \cdots \\ \cdot & \vdots & \cdot \end{bmatrix}_{m\times n} \begin{Bmatrix} \vdots \\ \begin{Bmatrix} B_n^R \\ B_n^D \\ B_n^F \\ D_n^F \end{Bmatrix}_{4\times1} \\ \vdots \end{Bmatrix}_{n\times1} = \begin{Bmatrix} \vdots \\ \left\{V_m^{asym}\right\}_{4\times1} \\ \vdots \end{Bmatrix}_{n\times1} \tag{35}$$

where

$$\left[W_{m,n}^{asym}\right]_{4\times4} =$$

$$\begin{bmatrix} 0 & J_{2n+1}(k_b\, b)N_{m,n} & -H_m^{(1)}(k_F\, b)Q_{m,n}(k_F d) & -H_m^{(2)}(k_F\, b)Q_{m,n}(k_F d) \\ 0 & T_{2n+1}(1, k_b\, b)N_{m,n} & -\dfrac{\mu_f}{\mu_D}T_m(3, k_F\, b)Q_{m,n}(k_F d) & -\dfrac{\mu_f}{\mu_D}T_m(4, k_F\, b)Q_{m,n}(k_F d) \\ H_m^{(1)}(k_s\, b_F)Q_{m,n}(k_s d) & 0 & H_m^{(1)}(k_F\, b_F)Q_{m,n}(k_F d) & H_m^{(2)}(k_F\, b_F)Q_{m,n}(k_F d) \\ T_m(3, k_s\, b_F)Q_{m,n}(k_s d) & 0 & \dfrac{\mu_f}{\mu_s}T_m(3, k_F\, b_F)Q_{m,n}(k_F d) & \dfrac{\mu_f}{\mu_s}T_m(3, k_F\, b_F)Q_{m,n}(k_F d) \end{bmatrix}_{4\times4} \tag{36}$$

$$\left\{V_m^{asym}\right\}_{4\times1} = \begin{Bmatrix} 0 \\ 0 \\ \varepsilon_m J_m(k_s\, b_F)\sin m\gamma\left[i^m \exp(-i\, k_s\, d\cos\gamma) - (-i)^m \exp(i\, k_s\, d\cos\gamma)\right] \\ \varepsilon_m R_m(1, k_s\, b_F)\sin m\gamma\left[i^m \exp(-i\, k_s\, d\cos\gamma) - (-i)^m \exp(i\, k_s\, d\cos\gamma)\right] \end{Bmatrix} \tag{37}$$

The displacement for the rigid-base model of the dike for driving motion $2u_0 \exp(-i\omega t)$ is

$$U^{(D)} = 2u_0 \frac{J_0(k_b R_1)}{J_0(k_b b)} \exp(-i\omega t) \tag{38}$$

3. RESULTS AND ANALYSIS

As dimensionless frequency we use

$$\eta = \frac{2a}{\beta_s T} = \frac{\omega a}{\pi \beta_s} \tag{39}$$

which is the ratio between the width of the wedge and the wavelength of shear waves in the half-space. If not indicated otherwise, the amplitude of the incident wave is $u_0 = 1$. The calculations were done using Matematica 4.0 interpreter on PC. We show results for a wedge softer than the half-space ($\mu_D / \mu_s = 1/16$ and $\rho_D / \rho_s = 1/4$), for a foundation thickness such that $b_F / b = 4/3$, and density such that $\rho_F / \rho_s = 1$. We vary the foundation rigidity, from $\mu_F / \mu_s = 1$ (same rigidity as the half-space) to $\mu_F / \mu_s = 50$ (stiff foundation compared to the half-space), and show how the results are affected by the stiffness of the foundation. The angle of the wedge is always $2\theta_0 = 150°$. In this paper, we illustrate how the relative stiffness of the foundation varies with μ_F / μ_s only. A more detailed and general study of the overall stiffness of the foundation for the model in Figure 1 would include dependence on ρ_F / ρ_s, ρ_D / ρ_s, μ_D / μ_s, and on the geometry of the foundation and its embedment (b_F / b and $2\theta_0$). We leave analyses of these dependences for future work.

3.1 Accuracy

A computational limitation of this method, based on expansion in cylindrical wave functions and requiring numerical solution of a truncated infinite system of equations, is that the system becomes singular for

number of terms in the series in eqns (18), (19), (22) and (24) grater than some value. The maximum number of terms (for which the system of equations is numerically stable) depends on dimensionless frequency, impedance contrasts, angle of incidence, and angle of the wedge, $2\theta_0$. The accuracy of the results also depends on the point where the motion is evaluated (the accuracy is the worst near lower corners of the wedge). For higher η, the maximum number of terms becomes too small for a desired accuracy to be achieved. In this paper, we show results for $\eta \le 1$, incident angle $\gamma = 0°$ and $45°$, and for angle of the wedge $2\theta_0 = 150°$. For smaller η, the results converge also for larger incident angles than $45°$ and for smaller wedge angle, but are not sufficiently accurate or diverge for $\eta = 1$ (see Figs 2 and 3 in Hayir et al., 2001).

Tables 1 and 2 show the upper bounds for the displacement and stress residuals, respectively along the contact surface between the wedge and the foundation and between the foundation and the half-space, for four values of η (= 0.25, 0.5, 0.75 and 1), for $\gamma = 0°$ and $90°$, and for three values of the ratio μ_F / μ_s ($=1$, 16 and 50). It can be seen that the error is the largest for $\eta = 1$, and along the boundary with the largest impedance contrast (wedge-foundation, for μ_F / μ_s=50).

Table 1 Upper bounds for normalized* displacement and stress residuals along the contact surface between the wedge and the foundation ($R_1 = b$), for unit amplitude incident waves, for a "soft" structure relative to the half-space ($\mu_D / \mu_s = 1/16$ and $\rho_D / \rho_s = 1/4$), and for three values of foundation stiffness relative to the one of the half-space.

$\mu_F / \mu_s = 1$, $\rho_F / \rho_s = 1$					
η	N	$\gamma = 0°$		$\gamma = 90°$	
		ε_U	ε_σ	ε_U	ε_σ
0.25	4	3.6×10^{-9}	6.1×10^{-8}	1.0×10^{-8}	9.2×10^{-9}
0.50	5	4.3×10^{-8}	5.8×10^{-7}	8.0×10^{-8}	1.8×10^{-6}
0.75	6	5.0×10^{-6}	1.3×10^{-4}	7.3×10^{-6}	2.3×10^{-4}
1.00	7	4.46×10^{-5}	1.4×10^{-3}	2.1×10^{-3}	7.5×10^{-2}
$\mu_F / \mu_s = 16$, $\rho_F / \rho_s = 1$					
η	N	$\gamma = 0°$		$\gamma = 90°$	
		ε_U	ε_σ	ε_U	ε_σ
0.25	3	7.8×10^{-8}	1.1×10^{-7}	2.1×10^{-5}	3.0×10^{-5}
0.50	4	2.7×10^{-5}	6.4×10^{-5}	7.6×10^{-4}	4.2×10^{-3}
0.75	5	1.2×10^{-3}	2.6×10^{-3}	1.1×10^{-1}	1.0×10^{-1}
1.00	5	3.0×10^{-4}	1.1×10^{-3}	3.2×10^{-3}	3.8×10^{-3}
$\mu_F / \mu_s = 50$ and $\rho_F / \rho_s = 1$					
η	N	$\gamma = 0°$		$\gamma = 90°$	
		ε_U	ε_σ	ε_U	ε_σ
0.25	3	2.1×10^{-6}	8.04×10^{-6}	3.3×10^{-4}	2.4×10^{-3}
0.50	4	3.1×10^{-3}	3.8×10^{-3}	1.1×10^{-1}	4.0×10^{-1}
0.75	4	2.8×10^{-4}	4.4×10^{-4}	7.7×10^{-3}	2.2×10^{-2}
1.00	5	4.7×10^{-2}	8.5×10^{-2}	1.3×10^{-4}	2.4×10^{-3}

* Normalization factor for displacements is the amplitude of the incident waves, u_0, and for the stresses is $\sigma_0 = \mu_D k_D u_0$.

Table 2 Upper bounds for normalized* displacement and stress residuals along the contact surface between the foundation and the half-space ($R_1 = b_F$), for unit amplitude incident waves, for a "soft" structure relative to the half-space ($\mu_D / \mu_s = 1/16$ and $\rho_D / \rho_s = 1/4$), and for two values of foundation stiffness relative to the one of the half-space.

$\mu_F / \mu_s = 16$, $\rho_F / \rho_s = 1$					
η	N	$\gamma = 0°$		$\gamma = 90°$	
		ε_U	ε_σ	ε_U	ε_σ
0.25	3	1.62×10^{-9}	4.6×10^{-11}	1.46×10^{-7}	1.84×10^{-7}
0.50	4	1.82×10^{-7}	8.03×10^{-8}	1.6×10^{-5}	2.6×10^{-5}
0.75	5	7.3×10^{-4}	2.0×10^{-3}	1.0×10^{-3}	3.0×10^{-3}
1.00	5	5.43×10^{-6}	4.81×10^{-6}	2.9×10^{-5}	6.6×10^{-5}
$\mu_F / \mu_s = 50$ and $\rho_F / \rho_s = 1$					
η	N	$\gamma = 0°$		$\gamma = 90°$	
		ε_U	ε_σ	ε_U	ε_σ
0.25	3	8.04×10^{-6}	8.28×10^{-6}	1.8×10^{-5}	2.4×10^{-5}
0.50	4	2.2×10^{-5}	6.9×10^{-5}	7.3×10^{-4}	2.0×10^{-3}
0.75	5	3.2×10^{-6}	4.02×10^{-6}	1.1×10^{-4}	3.9×10^{-4}
1.00	5	1.6×10^{-3}	3.5×10^{-3}	1.6×10^{-5}	2.48×10^{-5}

* Normalization factor for displacements is the amplitude of the incident waves, u_0, and for the stresses is $\sigma_0 = \mu_D k_D u_0$.

3.2 Transfer-Functions of the Soil-Foundation-Structure System Response

Although the lower boundary of the wedge is not closed (energy flows both ways through the contact surface with the foundation, and also through the contact surfaces between the foundation and the half-space), and its motion is not a superposition of its fixed-base frequencies, the motion of the system exhibits sharp variations near the fixed-base frequencies of the wedge. These frequencies can be determined from the representation of the wedge response by eqn (17), as the zeros of $J_n(k_D b)$, and those in the interval $\eta \in (0,1)$ are

η_n^{FB} = zeros of $J_n(k_D b)$			
n=0	n=1	n=2	n=3
0.37	0.58	0.78	0.98
0.85			

Which of these frequencies is seen in the response depends on the symmetry of the displacement amplitudes of the incident waves and of the location of the point where the response is evaluated. For example, for vertically incident waves, only the symmetric terms in the expansion in eqn (17) are excited, and the frequencies for n even only can be seen. For inclined incidence, both symmetric and anti-symmetric terms contribute to the response. However, even then, along the vertical axis of symmetry ($\theta_1 = 0$), $\sin\left[(2n+1)\frac{\pi}{2\theta_0}\theta_1\right]$=0 and only the terms with even n contribute to the response. At the top of the wedge, $R_1 = 0$ only the n=0 term contributes to the response (as $J_n = 0$ for $n \geq 1$).

Figure 2 shows the transfer-functions between the relative displacement at the top of the wedge, U^{rel}, and the average motion along the contact surface between the wedge and the foundation, U_{av}^{BOT}, and the incident wave, for a vertically incident wave. The relative wedge response on the top was evaluated as $U^{rel} = U^{TOP} - U_{av}^{BOT}$, where U^{TOP} is the absolute displacement of the top. The solid line corresponds to

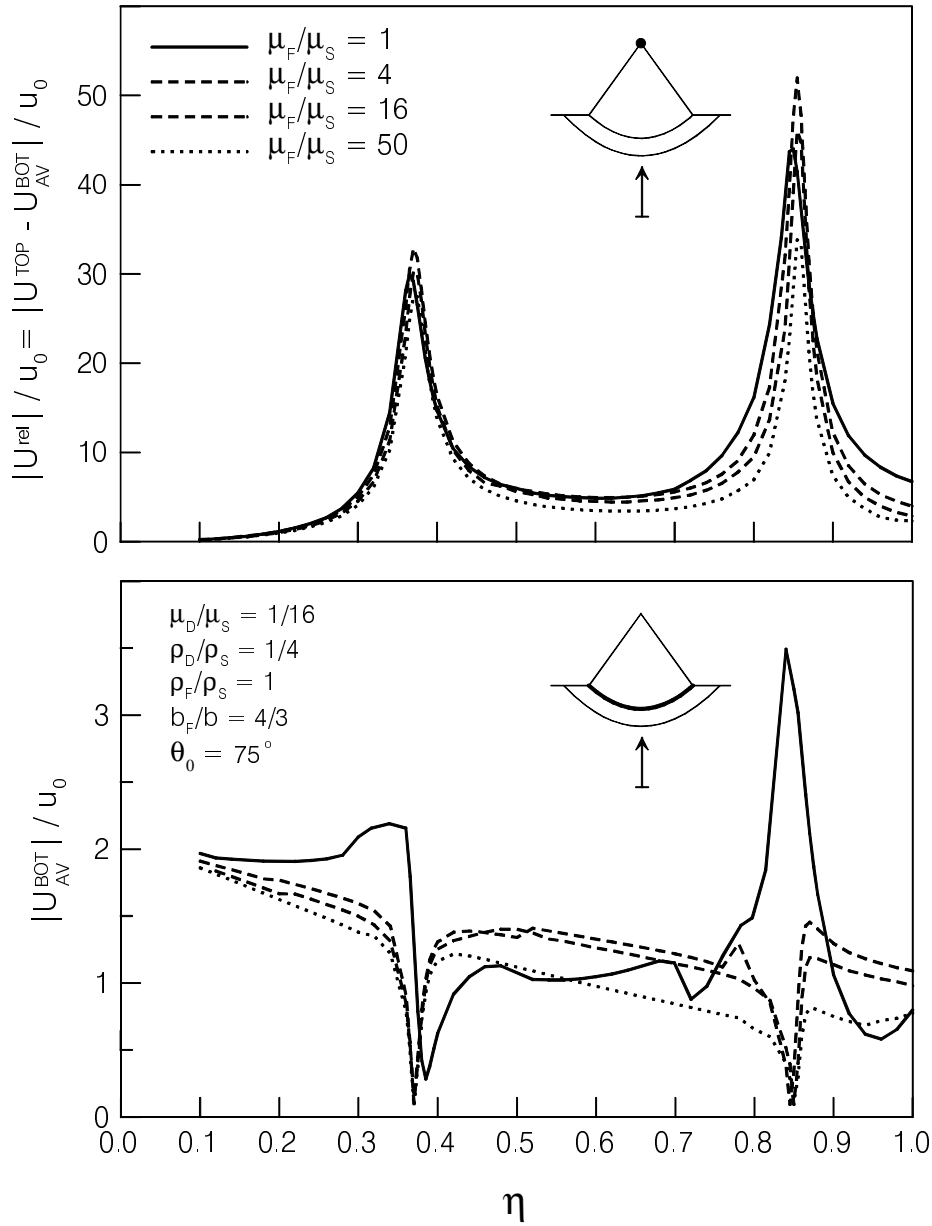

Figure 2 Top: Transfer-function between the displacement of the wedge top (relative to the average motion along the base) and the displacement of the incident wave for vertical incidence. Bottom: Transfer-function between the average displacement of the base of the wedge and the displacement of the incident wave for vertical incidence.

a foundation with same material properties as the half-space, and the segmented lines correspond to foundations with μ_F / μ_s = 4, 16 and 50. It can be seen that U^{rel} has distinctive peaks near the first and second zeroes of $J_0(k_D b)$ (near $\eta = 0.37$ and 0.85). The peaks are shifted towards higher frequencies for stiffer foundations, as the overall structure-foundation stiffness relative to the soil becomes larger. In the transfer-function for U_{av}^{BOT}, a small "peak" near the first zero of $J_2(k_D b)$ can also be seen (near $\eta = 0.78$). For stiffer foundations, the transfer-function of U_{av}^{BOT} looks very much like those published for rigid foundations (Trifunac, 1972). For a "surface" foundation (μ_F / μ_s =1), the transfer-function near the first fixed-base frequency is very similar to those for rigid foundations (has a sharp minimum), but near the second fixed-base frequency it has a peak and then a minimum. This figure also shows how the foundation filters progressively more of the high frequencies of the incident waves when it is stiffer relative to the soil (the backbone of the U_{av}^{BOT} amplitudes is smaller).

Figures 3a and b show the displacements on the free surface of the half space and along the base of the structure for a structure "softer" (bottom) and "harder" (top) than the half-space ($\mu_D / \mu_S = 50$ and 1/16 and $\rho_D / \rho_S = 1/4$ and 1), for two incident angles (γ = 0 and $45°$), and for the case when the foundation and half-space have same material properties, i.e. the structure is supported directly by the half-space. $|U|/u_0$ is shown for $-3 < x/a < 3$ and for $0.2 \le \eta \le 1.0$. It is seen that the displacement pattern is more complex for larger η and for $\gamma = 45°$ incidence. The displacement amplitudes on the half-space surface oscillate about the free-field amplitude (=2).

Figure 4 shows three-dimensional plots of the transfer-function between the motion along the base of the wedge (i.e. the contact surface between the wedge and the foundation) and the incident wave (with $\gamma = 45°$), extended to the left and to the right to include part of the foundation and half-space stress-free surface. The four surfaces correspond to different foundation rigidity, increasing progressively from left to right and from top to bottom. For softer foundation, (μ_F / μ_s =1 and 4), variations in the transfer-function associated with all the fixed-base frequencies listed above can be noticed, while for a very stiff foundation, noticeable are only variations associated with the frequencies for n=0 (i.e. the fixed-base frequencies excited by synchronous translation of the base. This figure can be used to infer how large the rigiditycontrast between the foundation and the soil should be for the common assumption made in soil-structure interaction modeling that the foundation is rigid is valid. This figure suggests that μ_F / μ_s should grater than about 20 (for $\rho_F / \rho_s = 1$). If the foundation is more flexible than that, soil-structure interaction models with a rigid-foundation assumption will not model the consequences of differential motion of the ground and may underestimate the stresses in the structure.

Figure 5 shows the transfer-functions between the motion of three points at the base of the wedge (left corner, mid point and right corner) and the incident wave, for the four values of foundation stiffness considered in Figures 2 and 4. This figure is included to explain further the relationship between variations of the three-dimensional surfaces shown in Fig. 4 and the fixed-base frequencies of the wedge. In the transfer-function for the left corner, variations can be noticed associated with all the five fixed-base frequencies of the wedge that fall within the frequency range considered. In the transfer-function for the mid point, variation associated only with the symmetric fixed-base modes are seen (two zeros of J_0 and one zero of J_2). In the transfer-function for the right corner, also there are variations associated with all the five fixed-base frequencies of the wedge (like for the left corner). The amplitudes are smaller because this point is in the "shadow" zone. However, the difference in amplitudes between the motion of the corner facing the incident wave and the one in the "shadow" zone diminishes when the foundation is very stiff.

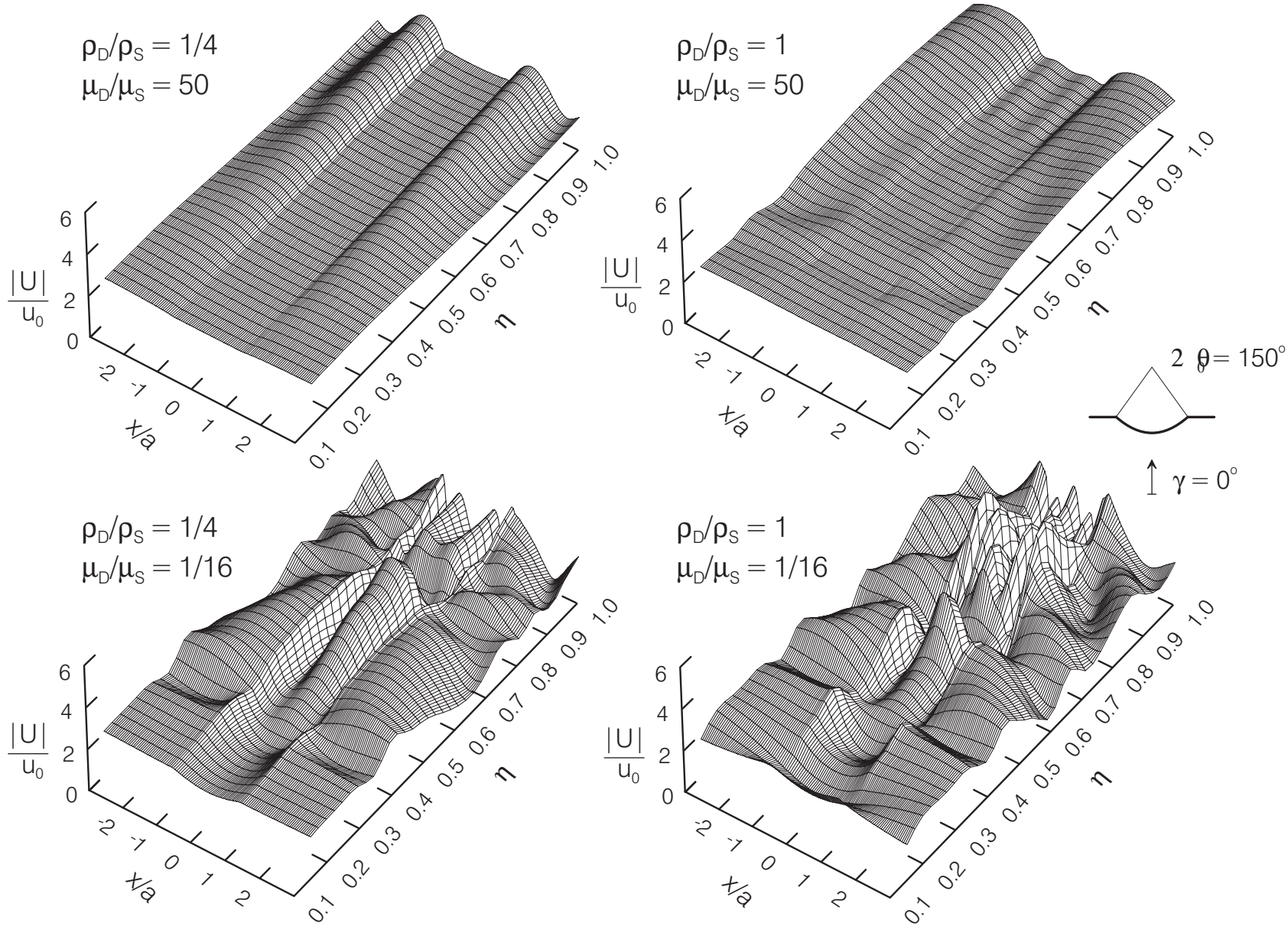

Fig. 3a Normalized displacements $|U| / u_0$ versus x/a and η, for a "stiff" structure ($\mu_D/\mu_S = 50$) and a "soft" structure ($\mu_D/\mu_S = 1/16$), for wedge angle $2\theta_0 = 150^o$ and for vertically incident waves.

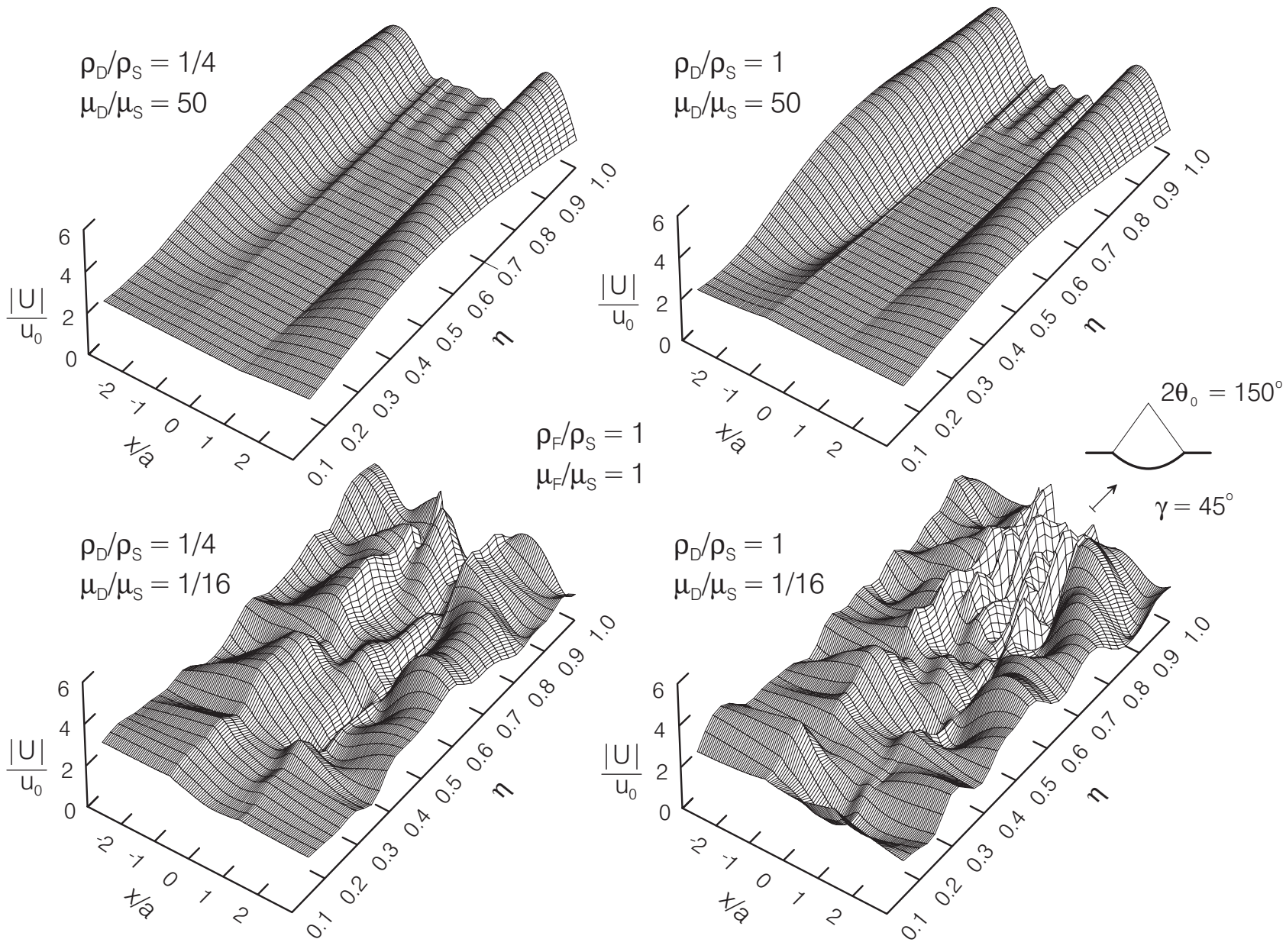

Fig. 3b Normalized displacements $|U| / u_0$ versus x/a and η, for a "stiff" structure ($\mu_D/\mu_S = 50$) and a "soft" structure ($\mu_D/\mu_S = 1/16$), for wedge angle $2\theta_0 = 150^o$ and incident angle $\gamma = 45^o$.

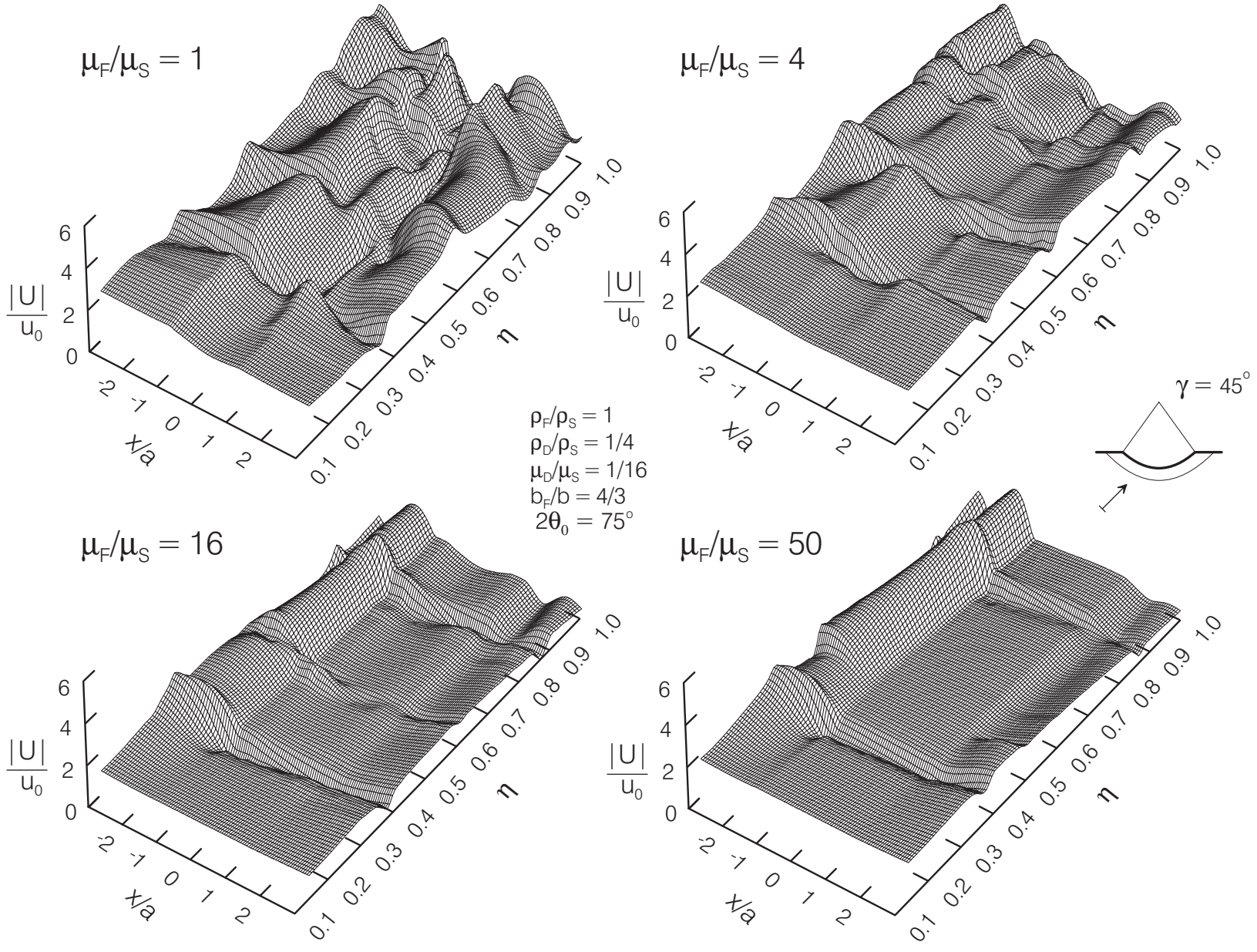

Fig. 4 Transfer-function of the displacement of the base of the wedge relative to the displacement of the incident wave, for incident angle $\gamma = 45^{o}$ and four values of the rigidity of the foundation relative to the soil (μ_F/μ_S = 1, 4, 16 and 50).

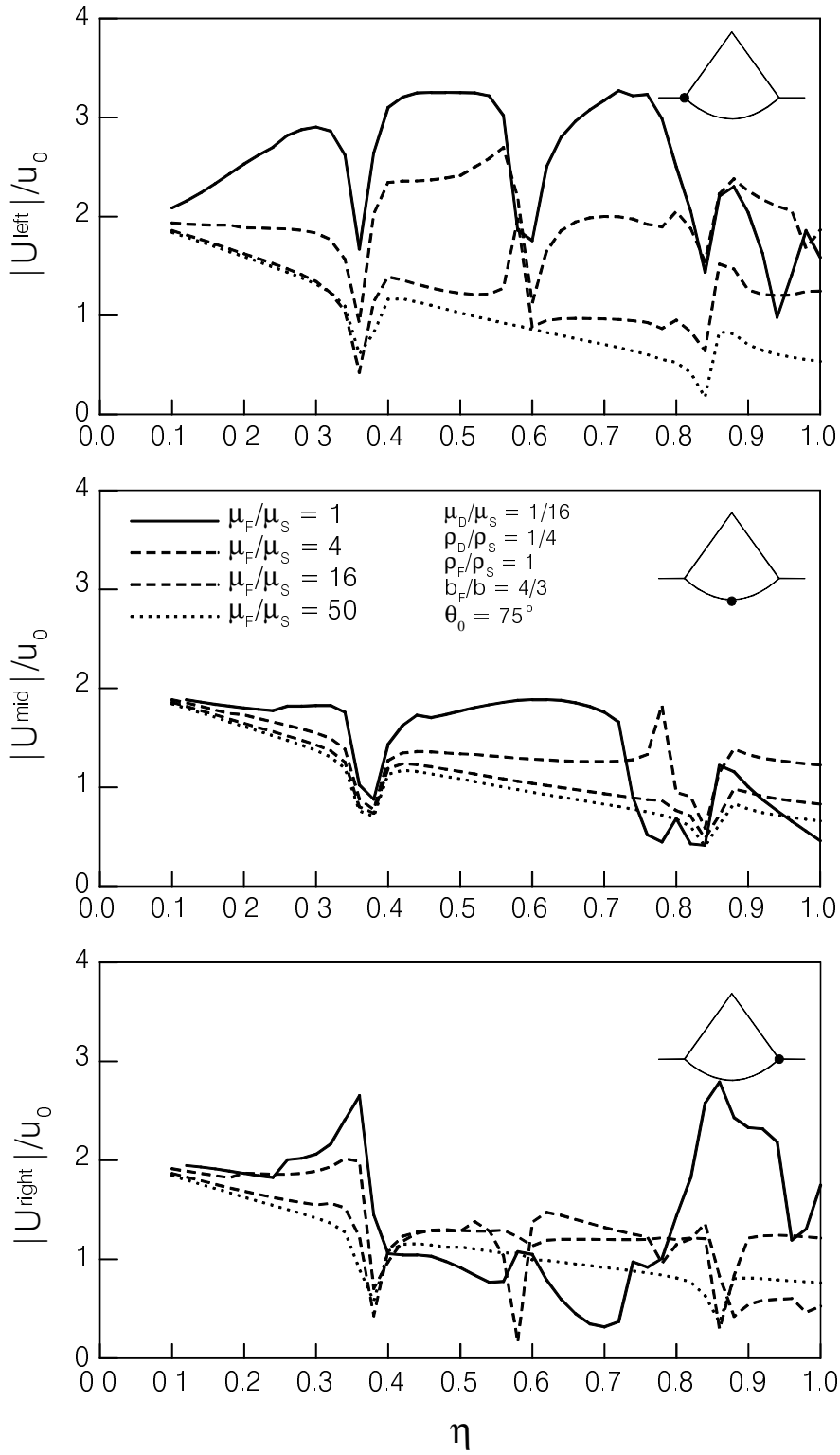

Figure 5 Transfer-functions of the displacement at three points on the base of the wedge (top: left corner, middle: mid point, bottom: right corner) relative to the displacement of the incident wave for incident angle $\gamma = 45°$. The different curves correspond to different rigidities of the foundation (μ_F / μ_s =1, 4, 16 and 50).

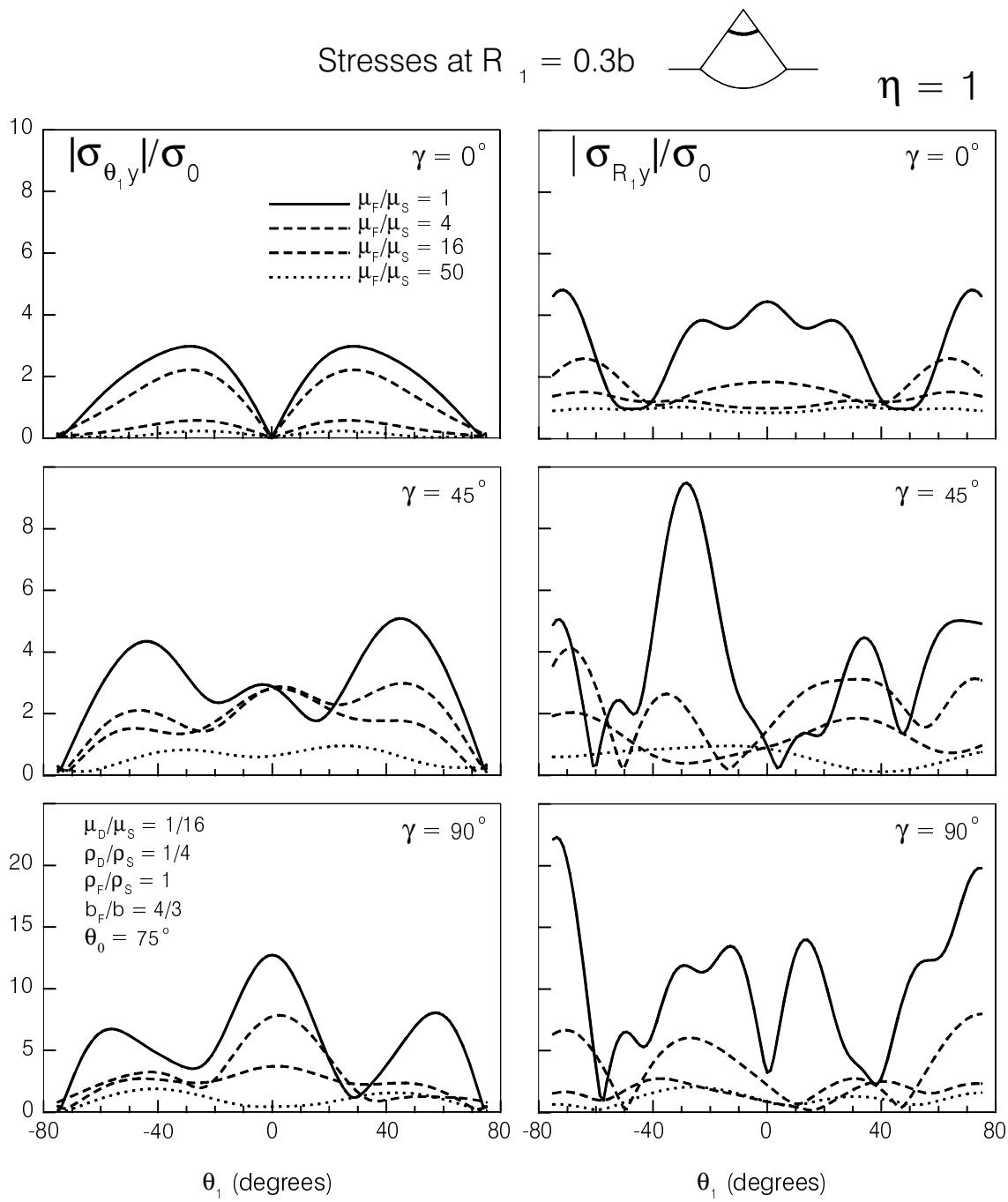

Figure 6 Stresses $\sigma_{\theta_1 y}^{(D)}$ (left) and $\sigma_{R_1 y}^{(D)}$ (right) in the wedge along $R_1 = 0.3b$, for dimensionless frequency $\eta = 1$ and incident angles $\gamma = 0°$, $45°$ and $90°$. The different curves correspond to four values of foundation rigidity relative to the soil: μ_F / μ_s =1, 4, 16 and 50.

3.3 Stresses due to Differential Motions

Differential motions of the base or individual supports of structures lead to additional stresses to those estimated assuming synchronous excitation of the base. For our model, shaken by synchronous excitation of the base, the stress $\sigma_{\theta_1 y}^{(D)} = 0$. In Figure 6 (left), we compare this stress evaluated along R_1=0.3b for different rigidities of the foundation $\mu_F / \mu_s = 1$, 4, 16 and 50. In Figure 6 (right), we show stress $\sigma_{R_1 y}^{(D)}$. The plots at the top middle and bottom correspond to incident angles $\gamma = 0°$, $45°$ and $90°$. In all plots, $\eta = 1$. It is seen that both stresses are of the same order of magnitude, and are small for a very stiff foundation, μ_F / μ_s=50, but not for a flexible foundation. The stress $\sigma_{R_1 y}^{(D)}$ is up to 10 times larger for μ_F / μ_s=1 than for μ_F / μ_s=50. Even for μ_F / μ_s=16, $\sigma_{R_1 y}^{(D)}$ can be about four times larger than for μ_F / μ_s=50.

4. CONCLUSIONS

A common assumption in soil-structure interaction analyses is that the foundation is rigid. This leads to ignoring differential ground motions and its effects on the structure. The validity of this assumption is difficult to tests due to the lack of adequate seismic instrumentation of structures documenting these deformations during strong earthquake shaking. Other models, on the other hand, consider differential motions but ignore the inertia interaction. In this paper, using a simple structural and foundation model, a circular wedge supported by a flexible foundation embedded into a half-space, both differential motions and soil-structure interaction are considered.

The question this paper attempted to answer is how rigid the foundation has to be, relative to the soil, for the rigid foundation assumption to be valid approximately. The results suggest that for μ_F / μ_s=50 the foundation behaves as rigid, but for μ_F / μ_s<16 it does not.

Considering differential motion is important for design, because of additional stresses caused by quazi-static deformations of the structure. The results in this paper show that, for a flexible foundation, the $\sigma_{\theta_1 y}^{(D)}$ stress in the structure is of the same order as $\sigma_{R_1 y}^{(D)}$ stress, while it is zero for fixed-base models and near zero for very stiff foundations, which reduce significantly the effects of differential ground motion. The results for the transfer-function of the average motion along the base of the structure show that flexible foundations are not efficient in scattering short wavelengths and thus do not shield the structure from being excited. This conclusion, reached for anti-plane incident waves, is in qualitative agreement with the one reached by Iguchi and Luco (1982) who computed impedances for a flexible disk foundation with a rigid core excited by in-plane incident waves.

ACKNOWLEDGEMENTS

The authors thank T.-Y. Hao for her help in preparation of the illustrations for this paper. Travel funds for presentation of this paper were provided by the Japanese International Science and Technology Exchange Center (JISTEC).

REFERENCES

1. Hayir, A., Todorovska, M.I. and Trifunac, M.D. (2001) Antiplane response of a dike with flexible soil-structure interface to incident SH-waves, *Soil Dynamics and Earthquake Engrg* (submitted for publication).
2. Todorovska, M.I., Hayir, A., and Trifunac, M.D. (2001) Antiplane response of a dike on a flexible embedded foundation to incident SH-waves, *Soil Dynamics and Earthquake Engrg* (submitted for publication).
3. Iguchi, M. and Luco, J.E. (1982). Vibration of flexible plate on visoelastic medium, *J. of Engng. Mech*., ASCE, **108**(6), 1103-1120.
4. Liou, G.-S. and Huang, P.H. (1994). Effects of flexibility on impedance functions for circular foundations, *J. of Engng. Mech*., ASCE, **120**(7), 1429-1446.
5. Todorovska, M.I., and V.W. Lee (1989). Seismic waves in buildings with shear walls or central core, ASCE, *J. of Engrg Mech.*, **115**(12), 2669-2686.
6. Todorovska, M.I., and M.D. Trifunac (1989). Antiplane earthquake waves in long structures, *J. of Engrg Mech.*, ASCE, **115**(12), 2687-2708.
7. Todorovska, M.I., and M.D. Trifunac (1990a). A note on the propagation of earthquake waves in buildings with soft first floor, *J. of Engrg Mech.*, ASCE, **116**(4), 892-900.
8. Todorovska, M.I., and M.D. Trifunac (1990b). A Note on excitation of long structures by ground waves, *J. of Engrg Mech*., ASCE, **116**(4), 952-964.
9. Trifunac, M.D. (1971). Surface motion of a semi-cylindrical alluvial valley for incident plane SH waves, *Bull. Seism. Soc. Am*., 61(2), 1755-1770.
10. Trifunac, M.D. (1972) Interaction of shear wall with the soil for incident Plane SH waves, Bull. Seism. Soc. Amec. 62, 63-83.
11. Trifunac, M.D., and M.I. Todorovska (1997). "Response spectra for differential motion of columns," *Earthquake Engrg and Struct. Dynam.*, **26**(2), 251-268.